

# HYCOT: A TRANSFORMER-BASED AUTOENCODER FOR HYPERSPECTRAL IMAGE COMPRESSION

Martin Hermann Paul Fuchs<sup>1</sup>, Behnood Rasti<sup>1,2</sup>, Begüm Demir<sup>1,2</sup>

<sup>1</sup>Faculty of Electrical Engineering and Computer Science, Technische Universität Berlin, Germany

<sup>2</sup>BIFOLD - Berlin Institute for the Foundations of Learning and Data, Germany

## ABSTRACT

The development of learning-based hyperspectral image (HSI) compression models has recently attracted significant interest. Existing models predominantly utilize convolutional filters, which capture only local dependencies. Furthermore, they often incur high training costs and exhibit substantial computational complexity. To address these limitations, in this paper we propose Hyperspectral Compression Transformer (HyCoT) that is a transformer-based autoencoder for pixelwise HSI compression. Additionally, we apply a simple yet effective training set reduction approach to accelerate the training process. Experimental results on the HySpecNet-11k dataset demonstrate that HyCoT surpasses the state of the art across various compression ratios by over 1 dB of PSNR with significantly reduced computational requirements. Our code and pre-trained weights are publicly available at <https://git.tu-berlin.de/rsim/hycot>.

**Index Terms**— Image compression, hyperspectral data, deep learning, transformer, remote sensing.

## 1. INTRODUCTION

Hyperspectral sensors acquire images with high spectral resolution, producing data across hundreds of observation channels. This extensive spectral information allows for detailed analysis and differentiation of materials based on their spectral signatures. However, the large number of spectral bands in hyperspectral images (HSIs) presents a significant challenge, namely the vast amount of data generated by hyperspectral sensors. While the volume of hyperspectral data archives is growing rapidly, transmission bandwidth and storage space are expensive and limited. To address this problem, HSI compression methods have been developed to efficiently transmit and store hyperspectral data.

Generally, there are two categories of HSI compression: i) traditional methods [1–3]; and ii) learning-based methods [4–8]. Most traditional methods are based on transform coding in combination with a quantization step and entropy coding. In contrast, learning-based methods train an artificial neural network (ANN) to extract representative features and

reduce the dimensionality of the latent space via consecutive downsampling operations.

Recent studies indicate that learning-based HSI compression methods can preserve reconstruction quality at higher compression ratios (CRs) compared to traditional compression methods [9]. Thus, the development of learning-based HSI compression methods has attracted great attention. The current state of the art in this field is formed by convolutional autoencoders (CAEs) [4–6]. The 1D-Convolutional Autoencoder (1D-CAE) model presented in [4] compresses the spectral content without considering spatial redundancies by stacking multiple blocks of 1D convolutions, pooling layers and leaky rectified linear unit (LeakyReLU) activations. Although high-quality reconstructions can be achieved with this approach, the pooling layers limit the achievable CRs to  $2^n$ . Another limitation of this approach is the increasing computational complexity with higher CRs due to the deeper network architecture. Unlike [4], to achieve spatial compression, Spectral Signals Compressor Network (SSCNet) that focuses on the spatial redundancies via 2D convolutional filters is introduced in [5]. In SSCNet, compression is achieved by 2D max pooling, while the final CR is adapted via the latent channels inside the bottleneck. With SSCNet much higher CRs can be achieved at the cost of spatially blurry reconstructions. To achieve joint compression of spectral and spatial dependencies, 3D Convolutional Auto-Encoder (3D-CAE) is introduced in [6]. 3D-CAE applies spatio-spectral compression via 3D convolutional filter kernels. Residual blocks allow gradients to flow through the network directly and improve the model performance. In general, CAEs fail to capture long-range spatial and spectral dependencies and their stacked convolutional layers make the architectures computationally expensive.

It is important to note that most of the deep learning models require large training sets to effectively optimize their parameters during training. On the one hand, training these models using large training sets allows them to generalize well. On the other hand, training often requires hundreds of epochs for model weight convergence [10], which results in high training costs. While training time can be reduced through parallelization on multiple GPUs, energy consumption and hardware requirements are still limiting factors.

To address these problems, we propose the Hyperspectral Compression Transformer (HyCoT) model that exploits a transformer-based autoencoder for HSI compression. HyCoT leverages long-range spectral dependencies for latent space encoding. For fast reconstruction, HyCoT employs a lightweight decoder. According to our knowledge, this is the first time a transformer-based model is investigated for HSI compression. To accelerate training while preserving reconstruction quality, we apply random sampling for reducing the training set. Experimental results demonstrate that HyCoT achieves higher reconstruction quality across multiple CRs, while reducing both training costs and computational complexity compared to state-of-the-art methods.

## 2. METHODOLOGY

Let  $\mathbf{X} \in \mathbb{R}^{H \times W \times C}$  be an HSI with image height  $H$ , image width  $W$  and  $C$  spectral bands. The objective of lossy HSI compression is to encode  $\mathbf{X}$  into a decorrelated latent space  $\mathbf{Y} \in \mathbb{R}^{\Sigma \times \Omega \times \Gamma}$  that represents  $\mathbf{X}$  with minimal distortion  $d : \mathbf{X} \times \hat{\mathbf{X}} \rightarrow [0, \infty)$  after reconstructing  $\hat{\mathbf{X}} \in \mathbb{R}^{H \times W \times C}$  on the decoder side.

To efficiently and effectively compress  $\mathbf{X}$ , we present HyCoT. HyCoT is a learning-based HSI compression model that employs the SpectralFormer [11] as a feature extractor on the encoder side, and a lightweight multilayer perceptron (MLP) for lossy reconstruction on the decoder side. Our model is illustrated in Figure 1. In the following subsections, we provide a comprehensive explanation of the proposed model.

### 2.1. HyCoT Encoder

The HyCoT encoder  $E_{\Phi} : \mathbf{X} \rightarrow \mathbf{Y}$  uses the SpectralFormer [11] as a backbone for spectral feature extraction. It aggregates long-range spectral dependencies via transformer blocks [12] inside a compression token (CT) and then projects the CT into the latent space using an MLP to fit the desired target CR.

In detail, each pixel  $\mathbf{x}$  of  $\mathbf{X}$  is processed separately. First, spectral groups  $\mathbf{g}^i$  are formed by nonoverlapping grouping of  $g_d$  neighbouring spectral bands, where  $g_d$  denotes the group depth. To make the number of bands divisible by  $g_d$ ,  $\mathbf{x}$  is padded from  $C$  to  $C_{\text{pad}} = C + \Delta_{\text{pad}}$ , forming  $\mathbf{x}_{\text{pad}}$ , where  $\Delta_{\text{pad}} = g_d - C \bmod g_d$ . The spectral groups are linearly projected to the embedding dimension  $d_{\text{emb}}$  using a learnable matrix  $\mathbf{P}$ . The resulting embedding vectors (so-called tokens) are defined as  $\tilde{\mathbf{t}}^i = \mathbf{P}\mathbf{g}^i$ . We propose prepending a learnable CT  $\tilde{\mathbf{t}}^0$ , which is also encoded by the transformer encoder to capture the spectral information of the pixel. The overall number  $n_t$  of tokens per pixel thus equals  $n_t = C_{\text{pad}}/g_d + 1$ . Afterwards, a learned position embedding  $\mathbf{l}^i$  is added to the patch embeddings to retain the positional information of the spectral groups as  $\mathbf{t}^i = \tilde{\mathbf{t}}^i + \mathbf{l}^i$ .

The sequence of tokens is then fed into the transformer encoder that stacks  $L$  transformer blocks. At each transformer block  $l = 1, \dots, L$ , multi-head self-attention (MSA) is applied followed by an MLP [12]. For both, a residual connection [13] is employed, followed by a layer normalization (LN) [14]:

$$\mathbf{t}'_l = \text{MSA}(\text{LN}(\mathbf{t}_{l-1})) + \mathbf{t}_{l-1}, \quad (1)$$

$$\mathbf{t}_l = \text{MLP}(\text{LN}(\mathbf{t}'_l)) + \mathbf{t}'_l, \quad (2)$$

where MSA is an extension of self-attention (SA) that runs  $k$  self-attention operations (heads) in parallel and projects their concatenated outputs [12]:

$$\text{MSA}(\mathbf{t}) = [\text{SA}_1(\mathbf{t}); \text{SA}_2(\mathbf{t}); \dots; \text{SA}_k(\mathbf{t})] \mathbf{U}_{\text{MSA}}. \quad (3)$$

SA computes a weighted sum over all values  $\mathbf{v}$  for each token  $\mathbf{t}$  and the attention weights  $\mathbf{A}_{ij}$  are based on the pairwise similarity between the query  $\mathbf{q}^i$  and key  $\mathbf{k}^j$  of two respective tokens [12]:

$$[\mathbf{q}, \mathbf{k}, \mathbf{v}] = \mathbf{t} \mathbf{U}_{\text{qkv}}, \quad (4)$$

$$\mathbf{A} = \text{softmax} \left( \frac{\mathbf{q}\mathbf{k}^T}{\sqrt{d_{\text{emb}}/k}} \right), \quad (5)$$

$$\text{SA}(\mathbf{t}) = \mathbf{A}\mathbf{v}. \quad (6)$$

The CT is extracted and sent to the MLP encoder that adapts the latent space channels  $\Gamma$  to fit the target CR. HyCoT compresses only the spectral content, and therefore the CR can be simplified as follows:

$$\text{CR} = \frac{C}{\Gamma}. \quad (7)$$

The MLP encoder initially applies a linear transformation of the CT with the embedding dimension  $d_{\text{emb}}$  to a hidden dimension  $d_{\text{hid}}$ , followed by a LeakyReLU to introduce non-linearity. Another linear transformation then adapts the CR by having  $\Gamma$  output features. Finally, the sigmoid activation function is applied to rescale the latent space.

### 2.2. HyCoT Decoder

The latent space  $\mathbf{Y}$  only consists of a few latent channels  $\Gamma$  per pixel. Consequently, a simple feedforward ANN with nonlinear activation functions is sufficient for a qualitative reconstruction. This enables fast decoding for real-time applications or frequent access to data archives with low latency. Thus, similar to the last block on the encoder side, the HyCoT decoder  $D_{\theta} : \mathbf{Y} \rightarrow \hat{\mathbf{X}}$  is lightweight and consists of only a simple MLP with one hidden dimension  $d_{\text{hid}}$  that upsamples the latent channel dimension  $\Gamma$  back to HSI input bands  $C$ . LeakyReLU is used after the initial layer and the sigmoid function after the hidden layer to scale the data back into the range 0–1 for the decoder output. Finally, the decoded pixels are reassembled to form the reconstructed image  $\hat{\mathbf{X}}$ .

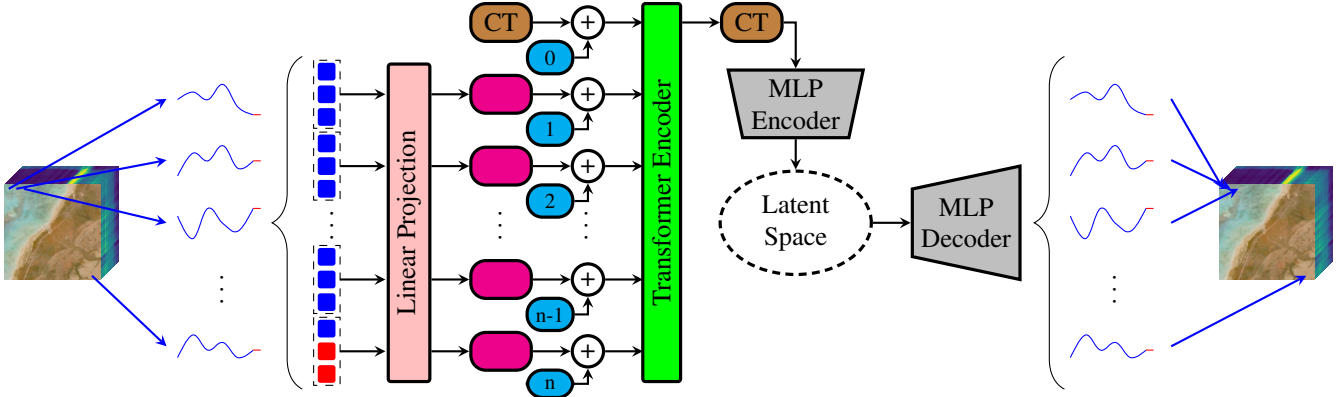


**Fig. 1.** Overview of our proposed HyCoT model. For each pixel of a given HSI, the spectral signature is padded. Neighbouring spectral bands are grouped and embedded by a linear projection [11] to form the transformer tokens. A CT is prepended and a learned position embedding is added. The sequence of tokens is fed into the transformer encoder [12]. Then, the CT is extracted and projected in the MLP encoder to fit the target CR. An MLP decoder is applied to reconstruct the full spectral signature. Finally, the decoded pixels are reassembled to form the reconstructed HSI.

### 3. EXPERIMENTAL RESULTS

The experiments were conducted on HySpecNet-11k [10] that is a large-scale hyperspectral benchmark dataset based on 250 tiles acquired by the Environmental Mapping and Analysis Program (EnMAP) satellite [15]. HySpecNet-11k includes 11,483 nonoverlapping HSIs, each of them having  $128 \times 128$  pixels and 202 bands with a ground sample distance of 30 m. Our code is implemented in PyTorch based on the CompressAI [16] framework. Training runs were carried out on a single NVIDIA A100 SXM4 80 GB GPU using the Adam optimizer [17]. For the HyCoT transformer encoder, we used  $d_{\text{emb}} = 64$ ,  $L = 5$  and  $k = 4$  as suggested in [11]. We empirically fixed the group depth  $g_d = 4$  and the hidden MLP dimension of both encoder and decoder to  $d_{\text{hid}} = 1,024$ .

#### 3.1. Training Set Reduction

Spectral information of pixels of the same material can be highly similar, leading to redundant information for the training stage of learning-based models. We aim to reduce the number of training samples by considering only a subset of the samples. To this end, we exploit random sampling within the training HSIs for efficiently reducing the training time. Instead of using all  $W \times H$  pixels of each training HSI  $\mathbf{X} \in \mathbb{R}^{H \times W \times C}$ , we only consider a fraction of that by randomly sampling  $n$  pixels of each HSI in each training epoch with  $n \ll W \cdot H$ . As a quantitative measure, we define the training set reduction factor  $r = \frac{W \cdot H}{n}$ . In this subsection, we analyse the efficiency of our suggested training set reduction approach. To this end, we fix  $r$  to have an optimal trade-off between training costs and reconstruction quality. In contrast to the training set, the test set is left unchanged to achieve comparable results.

To reduce the computational costs associated with training HyCoT from scratch for each  $r$ , we employed a new HySpecNet-11k split, denoted as the mini split. The mini split represents a condensed version of HySpecNet-11k, which we recommend to use for hyperparameter tuning. To obtain the mini split, we followed [10] and divided the dataset randomly into i) a training set that includes 70% of the HSIs, ii) a validation set that includes 20% of the HSIs, and iii) a test set that includes 10% of the HSIs. However, the mini split only uses the center HSI of each tile used to create HySpecNet-11k. This selection strategy reduces the dataset size to 250 HSIs, while maintaining the global diversity of HySpecNet-11k (11,483 HSIs).

Table 1 shows the results of training HyCoT for the highest considered CR = 28.86 on the HySpecNet-11k mini split using different  $r$ . For this experiment, the HyCoT models were trained for 1,000 epochs with a learning rate of  $10^{-4}$ . The table shows that reconstruction quality can be preserved when training with a randomly subsampled training set. In detail, reconstruction quality for  $r = 64$  is slightly higher than considering the complete training set ( $r = 1$ ). This indicates high redundancy among the pixels within the training set, suggesting that not all pixels are necessary to achieve robust generalization performance. We would like to note that even higher values of  $r$  can be considered for even further training cost reduction at a slightly reduced reconstruction quality.

#### 3.2. Rate-Distortion Evaluation

In this subsection, we analyse the rate-distortion curves of learning-based HSI compression models. Our experimental results are shown in Figure 2. To achieve these results, we used the HySpecNet-11k easy split as proposed in [10].

**Table 1.** HyCoT trained on HySpecNet-11k (mini split) with different values of the training set reduction factor  $r$  for a fixed CR of 28.86. Reconstruction quality is evaluated as PSNR on the test set.

$r$	PSNR [dB]
1	45.612
4	45.550
16	45.344
64	<b>45.669</b>
256	45.193
1,024	44.886
4,096	44.509
16,384	43.977

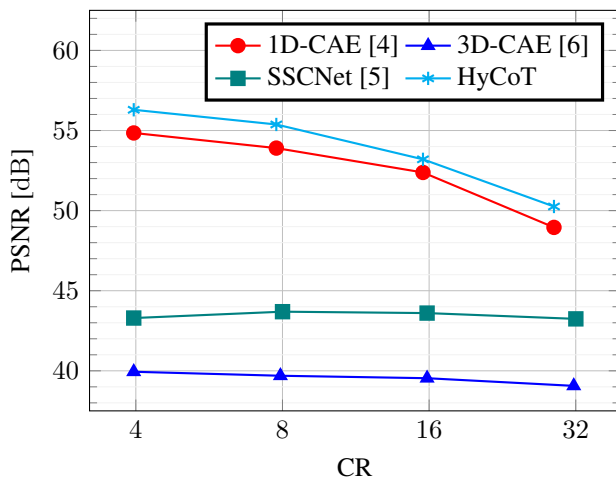


**Fig. 2.** Rate-distortion performance on the test set of HySpecNet-11k (easy split).

We used mean squared error (MSE) as a loss function until convergence on the validation set, which was achieved after 2,000 epochs for each experiment using a learning rate of  $10^{-3}$ . We trained HyCoT, targeting the four specific CRs of 1D-CAE [4], to make our results comparable to the baseline. We would like to note that HyCoT is more versatile in terms of CR, see (7), than CAEs since HyCoT is not based on strided convolutions or pooling operations. For the HyCoT results, we significantly reduced the training costs by a factor of  $r = 64$ . Yet, HyCoT is able to outperform all CAE baselines at every CR, which were trained on the full training set. Quantitatively, HyCoT is at least 1 dB better than 1D-CAE for each CR while for  $CR \approx 4$  outperforming SSCNet and 3D-CAE with 13.00 dB and 16.36 dB, respectively. This shows that one-dimensional spectral dimensionality reduction is beneficial for HSI compression and that long-range spectral dependencies, which are captured inside the transformer encoder of HyCoT, are relevant for high quality reconstruction.

**Table 2.** Computational complexity analysis. FLOPs are calculated using a HySpecNet-11k HSI of size  $128 \times 128$  pixels.

Model	CR	FLOPs	Parameters
1D-CAE [4]	3.96	176.64 G	<b>56,130</b>
SSCNet [5]	4.00	84.18 G	34,136,586
3D-CAE [6]	3.96	121.40 G	933,539
HyCoT	3.96	<b>6.82 G</b>	488,225
1D-CAE [4]	7.77	719.94 G	<b>238,018</b>
SSCNet [5]	8.00	76.56 G	19,240,298
3D-CAE [6]	7.92	104.68 G	677,443
HyCoT	7.77	<b>5.98 G</b>	437,000
1D-CAE [4]	15.54	2,840.00 G	962,242
SSCNet [5]	16.00	72.74 G	11,792,154
3D-CAE [6]	15.84	96.32 G	549,395
HyCoT	15.54	<b>5.54 G</b>	<b>410,363</b>
1D-CAE [4]	28.86	12,180.00 G	3,852,482
SSCNet [5]	32.00	70.84 G	8,068,082
3D-CAE [6]	31.69	92.16 G	485,371
HyCoT	28.86	<b>5.34 G</b>	<b>398,069</b>

### 3.3. Computational Complexity Analysis

In this subsection, we compare the computational complexity of HyCoT with those of other models. In Table 2 we report a comparison of the floating point operations (FLOPs) and the number of model parameters for multiple CRs. From the table, one can see that for low CRs, 1D-CAE [4] has few parameters. However, by increasing CR, the parameters rise exponentially, since the network stacks up layers with each added downsampling operation. The high FLOPs of 1D-CAE are due to the pixelwise convolutional processing. In contrast, the computational complexity of HyCoT decreases by increasing CRs since the transformer encoder backbone stays the same and only the output channels of the MLP encoder are slimmed, when compressing to a smaller latent space. Thus, HyCoT results in a faster runtime. In addition, increasing the CR reduces the number of parameters compared to 1D-CAE, where the opposite is the case. It is worth mentioning that the lightweight decoder of HyCoT is suitable for real-time HSI reconstruction. We also report the computational complexity for SSCNet and 3D-CAE in the table. SSCNet and 3D-CAE are associated to higher parameter counts and FLOPs due to their multi-dimensional convolutional layers and therefore cannot compete with our HyCoT model.

## 4. CONCLUSION

In this paper, we have proposed the Hyperspectral Compression Transformer (HyCoT) model. HyCoT compresses hyperspectral images using a transformer-based autoencoder to leverage long-range spectral dependencies. To enhance training efficiency, we have exploited only a small, randomized subset of the available training set in each epoch. Exper-

imental results have shown the efficiency of our proposed model in both training time and computational complexity, while also surpassing state-of-the-art convolutional autoencoders in terms of reconstruction quality for fixed compression ratios. As future work, we plan to extend our HyCoT model to achieve efficient spatio-spectral compression and explore a strategy for selecting informative training samples.

## 5. REFERENCES

- [1] S. Lim, K. Sohn, and C. Lee, "Compression for hyperspectral images using three dimensional wavelet transform," *IEEE International Geoscience and Remote Sensing Symposium*, vol. 1, pp. 109–111, 2001.
- [2] B. Penna, T. Tillo, E. Magli, and G. Olmo, "A new low complexity KLT for lossy hyperspectral data compression," *IEEE International Symposium on Geoscience and Remote Sensing*, pp. 3525–3528, 2006.
- [3] Q. Du and J. E. Fowler, "Hyperspectral image compression using JPEG2000 and principal component analysis," *IEEE Geoscience and Remote Sensing Letters*, vol. 4, no. 2, pp. 201–205, 2007.
- [4] J. Kuester, W. Gross, and W. Middelmann, "1D-convolutional autoencoder based hyperspectral data compression," *International Archives of Photogrammetry, Remote Sensing and Spatial Information Sciences*, vol. 43, pp. 15–21, 2021.
- [5] R. La Grassa, C. Re, G. Cremonese, and I. Gallo, "Hyperspectral data compression using fully convolutional autoencoder," *Remote Sensing*, vol. 14, no. 10, p. 2472, 2022.
- [6] Y. Chong, L. Chen, and S. Pan, "End-to-end joint spectral–spatial compression and reconstruction of hyperspectral images using a 3D convolutional autoencoder," *Journal of Electronic Imaging*, vol. 30, no. 4, p. 041403, 2021.
- [7] N. Sprengel, M. H. P. Fuchs, and B. Demir, "Learning-based hyperspectral image compression using a spatio-spectral approach," *EGU General Assembly*, 2024.
- [8] Y. Guo, Y. Chong, and S. Pan, "Hyperspectral image compression via cross-channel contrastive learning," *IEEE Transactions on Geoscience and Remote Sensing*, vol. 61, pp. 1–18, 2023.
- [9] A. Altamimi and B. Ben Youssef, "A systematic review of hardware-accelerated compression of remotely sensed hyperspectral images," *Sensors*, vol. 22, no. 1, p. 263, 2021.
- [10] M. H. P. Fuchs and B. Demir, "HySpecNet-11k: A large-scale hyperspectral dataset for benchmarking learning-based hyperspectral image compression methods," *IEEE International Geoscience and Remote Sensing Symposium*, pp. 1779–1782, 2023.
- [11] D. Hong, Z. Han, J. Yao, L. Gao, B. Zhang, A. Plaza, and J. Chanussot, "SpectralFormer: Rethinking hyperspectral image classification with transformers," *IEEE Transactions on Geoscience and Remote Sensing*, vol. 60, pp. 1–15, 2021.
- [12] A. Vaswani, N. Shazeer, N. Parmar, J. Uszkoreit, L. Jones, A. N. Gomez, Ł. Kaiser, and I. Polosukhin, "Attention is all you need," *Advances in Neural Information Processing Systems*, vol. 30, 2017.
- [13] K. He, X. Zhang, S. Ren, and J. Sun, "Deep residual learning for image recognition," *IEEE Conference on Computer Vision and Pattern Recognition*, pp. 770–778, 2016.
- [14] J. L. Ba, J. R. Kiros, and G. E. Hinton, "Layer normalization," *arXiv preprint arXiv:1607.06450*, 2016.
- [15] L. Guanter, H. Kaufmann, K. Segl, S. Foerster, C. Rogass, S. Chabrillat, T. Kuester, A. Hollstein, G. Rossner, C. Chlebek *et al.*, "The EnMAP spaceborne imaging spectroscopy mission for earth observation," *Remote Sensing*, vol. 7, no. 7, pp. 8830–8857, 2015.
- [16] J. Bégin, F. Racapé, S. Feltman, and A. Pushparaja, "CompressAI: A pytorch library and evaluation platform for end-to-end compression research," *arXiv preprint arXiv:2011.03029*, 2020.
- [17] D. P. Kingma and J. Ba, "Adam: A method for stochastic optimization," *arXiv preprint arXiv:1412.6980*, 2014.